LBL-18706
c.2

LBL-18706
Preprint

Submitted to the Journal of
the American Ceramic Society

THE EFFECT OF SHEAR STRESS ON SINTERING

M.N. Rahaman, L.C. De Jonghe,
and R.J. Brook

November 1984

RECEIVED
LAWRENCE
BERKELEY LABORATORY

JAN 7 1985

LIBRARY AND
DOCUMENTS SECTION

TWO-WEEK LOAN COPY

*This is a Library Circulating Copy
which may be borrowed for two weeks.*

Lawrence Berkeley Laboratory
University of California
Berkeley, California 94720

Prepared for the U.S. Department of Energy
under Contract DE-AC03-76SF00098

Center for Advanced Materials

LBL-18706
c.2

DISCLAIMER

This document was prepared as an account of work sponsored by the United States Government. While this document is believed to contain correct information, neither the United States Government nor any agency thereof, nor the Regents of the University of California, nor any of their employees, makes any warranty, express or implied, or assumes any legal responsibility for the accuracy, completeness, or usefulness of any information, apparatus, product, or process disclosed, or represents that its use would not infringe privately owned rights. Reference herein to any specific commercial product, process, or service by its trade name, trademark, manufacturer, or otherwise, does not necessarily constitute or imply its endorsement, recommendation, or favoring by the United States Government or any agency thereof, or the Regents of the University of California. The views and opinions of authors expressed herein do not necessarily state or reflect those of the United States Government or any agency thereof or the Regents of the University of California.

LBL - 18706

THE EFFECT OF SHEAR STRESS ON SINTERING

M. N. Rahaman* and L. C. De Jonghe*
Center for Advanced Materials
Lawrence Berkeley Laboratory
and
Department of Materials Science and Mineral Engineering
University of California
Berkeley, CA 94720

R. J. Brook*
Department of Ceramics
The University of Leeds
Leeds LS2 9JT. England

*Member, American Ceramic Society

This work was supported by the Division of Materials Science, Office of Basic Energy Sciences, U.S. Department of Energy, under Contract No. DE-AC03-76SF00098.

ABSTRACT

The effect of small uniaxial stresses on the sintering of CdO powder compacts was studied using a loading dilatometer. Compacts of two different green densities were sintered at 1123K and subjected to stresses between 0 and 0.25 MPa. Densification and creep occurs simultaneously and the effects of these two processes can be separated. Between relative densities of 0.5 and 0.9, the dependence of the uniaxial creep rate on density can be described in terms of a stress intensity factor which depends exponentially on the porosity but is independent of the grain size. Comparison of the densification and the creep rates permits the definition of the sintering stress, which is found to decrease with increasing density, and verification of the Zener relationship. The stress and grain size dependence of the creep rate, and the grain size dependence of the densification rate, support grain boundary diffusion as the rate controlling step in both processes.

INTRODUCTION

Inhomogeneities such as agglomerates, particle size distribution and spatial density variations in a powder compact can lead to differential sintering rates which, in turn, produce stresses.[1] These stresses give rise to creep. Thus a compact containing inhomogeneities will experience creep and densification simultaneously during sintering. To understand such sintering behaviour, it is required, first, to understand both processes and second, to examine how they affect one another when they occur simultaneously. In an earlier publication,[2] two of the present authors showed how the second step could be accomplished with a loading dilatometer which applies a measured, small uniaxal stress during densification.

This paper seeks to extend the study in both experimental and theoretical areas. CdO powder compacts were sintered under low uniaxial stresses between 0 and 0.25 MPa at 1123K. The results were compared with the predictions of existing models and then used to explore the functional dependence of the effective stress in creep and the sintering stress in densification on density and grain size.

A key question in simultaneous creep and densification is the influence of the changing density on the creep rate, i.e., the influence of pores. This has traditionally been treated by the use of a stress concentration term, ϕ, usually referred to as the stress intensity factor which is the ratio of the cross-sectional area of the specimen, A, over its actual, internal load-bearing area, A_e; i.e $\phi = A/A_e$. After long debate, Coble[3] proposed that $\phi = 1/\rho$, where ρ is the

relative density, for the intermediate and final stages of densification. Beere[4,5] calculated ϕ for a model in which a more elaborate pore/boundary geometry was considered. Viera and Brook[6] have shown that Beere's results may be fitted to an expression of the form $\phi = \exp(\alpha P)$, where α depends on the equilibrium dihedral angle and P is the porosity. Raj and Bordia[7] have recently developed a phenomenological theory for the sintering of bimodal powder compacts consisting of two regions which sinter at different rates. The model consists of two Hookean springs and a Newtonian viscous dashpot arranged to form a standard linear solid. The assumption of a Newtonian viscous dashpot, while allowing analytical solutions of the equations, is equivalent to the use of ϕ = constant. An significant result of Raj and Bordia's model, however, is that certain material properties, such as the densification rate and the initiation of cracks in the sintering compact, are sensitive to the ratio of the creep rate to the densification rate in the two regions of the bimodal compact.

The sintering stress, Σ, is a fundamental parameter in the understanding of the densification process. Its measurement and its dependence on variables such as density and grain size are therefore of considerable importance. Very little work has been performed in this area. Gregg and Rhines[8] proposed a relation for the sintering stress Σ, of the form $\Sigma = \alpha\gamma PH$, where α is a proportionality factor taken to be 1, γ is the surface tension, P is the porosity and H the mean curvature of the pore surface. They measured Σ for copper powder compacts as the uniaxial stress needed to stop uniaxial shrinkage and

found, surprisingly, that Σ increased with density up to ~0.95 relative density. This increase was attributed to an increase in pore surface cuvature.[9]

The work of Gregg and Rhines also showed that Σ is inversely proportional to the starting grain size. Beere's model[4,5] predicts that Σ is inversely proportional to grain size but its relation to density is very complicated. However, for very large dihedral angles (180 degrees), Σ would be relatively constant between relative densities of 0.5 to 0.9.

EXPERIMENTAL PROCEDURE

CdO powder* compacts (6mm by 6mm) of two different green densities were used in the present work. Compacts having a green density of ρ_0 = 0.58±0.01 of the theoretical density were made by uniaxially compaction the powder at 20 MPa in a tungsten carbide die followed by isostatic pressing at 68 MPa. Compacts having a lower green density ρ_0 = 0.39± 0.01 were made by uniaxially pressing the powder at 12MPa. These two green densities were used in order to cover a wide range of sintered density. The compacts were sintered in flowing air (50 cm^3/min) for two hours in a loading dilatometer. The instrument and its associated control and monitoring equipment are described in detail elsewhere.[2,10] Sintering was performed at 1123K and under low uniaxial stresses between 0 and 0.25 MPa. The sintering procedure was the same as that described recently.[2] The mass and dimensions of the compacts were measured before and after sintering and the final density measured using Archimedes' Principle.

In a separate set of experiments sintering was terminated after times between 0 and 2 hours and the dimensions of these compacts measured using a micrometer. Fracture surfaces and polished surfaces of these compacts were examined using scanning electron microscopy and the micrographs obtained were used to determine average grain sizes and the equilibrium dihedral angle.

RESULTS

Fig. 1 shows results for the axial shrinkage, $\Delta L/L_0$ versus the logarithm of time, log t, for applied loads between 0 and 5N and for two different green densities, $\rho_0 = 0.58$ and $\rho_0 = 0.39$, respectively. (L_0 = initial sample length, $\Delta L = L - L_0$, where L = instantaneous sample length). Results for loads of 2N and 4N have been omitted from some figures for clarity. A load of 1N represents a stress of 45 kPa and t = 0 represents the commencement of shrinkage. The sintering temperature was reached after t = 8 min. Each curve is the average of two runs under the same conditions. The curves were reproducible to within ±2%. Weight losses after sintering for 2 hours were ~0.7% and ~1% for the higher and lower green density compacts, respectively, and the applied loads could be maintained to ±5%. It is seen that at any time, $\Delta L/L_0$ and the effect of load on $\Delta L/L_0$ are both enhanced for the lower green density compact.

The application of load causes anisotropic shrinkage of the compact. This is shown in fig. 2 where the axial shrinkage, $\Delta L/L_0$, is plotted versus the radial shrinkage, $\Delta D/D_0$, between t ~10 and t = 120

minutes. (D_0 = initial sample diameter, $\Delta D = D-D_0$, where D = instantaneous sample diameter). $\Delta L/L_0$ is approximately proportional to $\Delta D/D_0$ for both the lower and the higher green density compacts. For any green density, the slopes of the lines increase with increasing load, and for any load, the degree of anisotropic shrinkage is higher for the lower green density compact.

A methodology described by Raj,[11] and figures 1 and 2 were used to separate the creep strain, ε, from the strain due to densification. Fig. 3 shows the results for ε versus log t. Between t ~ 10 and t ~ 120 minutes, ε varies approximately linearly with log t. The slopes of the curves increase with increasing load and at any time, the lower green density compact creeps faster than the higher green density compact. In addition the creep rate of the lower density compact increases linearly with applied stress, as found earlier[1] for the higher green density compact.

Fig. 4 shows the results for the relative density, ρ versus log t. ρ increases approximately linearly with log t for both curves and applied load has no effect on ρ. It is also seen that the two curves are almost parallel and this suggests that the densification rate at time t is almost independent of the initial compact density, ρ_0. The final densities calculated from the sintering curves are in good agreement with the values determined by using Archimedes' Principle.

Fig. 5 shows scanning electron micrographs of the fracture surfaces of two compacts (ρ_0 = 0.58) sintered for (A), t = 20 and (B),

t = 120 min. respectively. It is clear that grain growth has occurred. There is also a certain amount of grain faceting at longer times, as seen from fig. 5 (B). Average grain sizes were determined from fracture surfaces between t = 10 and t = 120 min, and these follow a cubic grain growth law of the form $(G/G_0)^3 = 1 + t/4$, where G_0 is the average grain size at the commencement of shrinkage (t = 0). The average grain sizes for the lower green density compacts appear to follow the same law, since at t = 20 and at t = 120 min., the average grain size of the lower green density compact was the same as that for the higher green density compact. Thus, grain growth rates were independent of porosity.

Equilibrium dihedral angles were measured from scanning electron micrographs of a polished surface of a higher green density compact sintered to a relative density of ~ 0.88. The mean value obtained was ~ 120 degrees.

DISCUSSION

A key benefit of these experiments is the ability to observe the simultaneous effect of uniaxial creep and densification and to separate these. These effects are discussed separately in the following sections.

(i) **Creep Rate:**

In the analysis of the creep results of fig. 3, the logarithm of the creep rate, log $\dot{\varepsilon}$, was plotted versus the relative density, ρ. This is shown in fig. 6 for three different loads for compacts of

green densities $\rho_0 = 0.39$ and $\rho_0 = 0.58$ respectively. The curves are approximately parallel to one another and decrease markedly, but linearly, with increasing ρ. This shows that $\dot{\varepsilon}$ has an exponential dependence on ρ (or on the porosity, P).

It can be seen that $\dot{\varepsilon}$ for the low green density compact at $\rho = 0.7$ is very much lower than that for the high green density compact. An explanation for this is linked to the strong grain size dependence of $\dot{\varepsilon}$ for diffusional creep behaviour and to the opportunity for grain growth in the low green density compact as it sinters up to $\rho = 0.7$.

To compensate for grain growth, use may be made of an equation for the creep rate, of the general form

$$\dot{\varepsilon} = \frac{CD\Omega\delta_e^p}{X_o^m \, k_B \, T} \qquad \text{Eqn. (1)}$$

where X_0 is the radius of a load-bearing grainboundary area between two grains, C is a constant defined by the geometry, D is the diffusivity, Ω is the molecular volume, k_B is the Boltzmann constant, T is the absolute temperature, δ_e is the effective mean stress on the grain boundaries, and m and p are exponents characteristic of the mechanism of creep. For diffusion controlled creep p = 1. m = 2 for lattice diffusion (Nabarro-Herring Creep[12,13]) and m = 3 for grain boundary diffusion (Coble creep[14]). Since $X_0 = G(A_e / A)^{1/2} = G/\phi^{1/2}$, Eqn.1 reduces to

$$\dot{\varepsilon} = K_1 \delta_e^p \, \phi^{m/2} / \, G^m \qquad \text{Eqn (2)}$$

As shown earlier[2] for these results $p = 1$. Compensation for grain growth can be made by use of the plot $\log (G^m\dot{\varepsilon})$ versus ρ, where the values for the grain size, G, at time t corresponding to ρ (at time t) follow from

$$(G/G_0)^n = 1 + kt \qquad \text{Eqn (3)}$$

where G and G_0 are the grain sizes at times t and t = 0 respectively, and n and k are constants. When the logarithm of the grain size compensated creep rate* $\log (G^m\dot{}/G_0^m)$ is plotted versus ρ, as shown in fig. 6, the results are brought onto one common line, for both ρ_0 = 0.39 and ρ_0 = 0.58, when the value for m is equal to 3 (Coble creep). Use of m = 2 (Nabarro-Herring creep) fails to remove the grain growth effect resulting from the different green densities, emphasizing that m = 3 is indeed the correct choice for the grain size dependence of the creep rate. This common line of $\log G^m\dot{\varepsilon}/G_0^m$ versus ρ follows from Eqn. 2 for proper choice of m, when ϕ does not depend on grain size. Since both data sets begin with the same grains size, this line should intersect the data at $\rho = \rho_0$ if indeed ϕ is independent of grain size. This is very nearly the case, as shown in Fig. 6. The constants in equation 2, $n = 3.0 \pm 0.1$ and $k = 0.25\ \text{min}^{-1}$, are in good agreement with those derived experimentally from scanning electron micrographs of fracture surfaces.

*Note that $\log G^m\dot{\varepsilon}/G_0^m$ is plotted instead of $\log(G^m\dot{\varepsilon})$. Use of the G_0 term, while only shifting the curves vertically, simplifies the treatment of the data.

The exponents P = 1 and m = 3 in Eqn. 1 strongly suggest that the creep process is accomodated by grain boundary diffusion. Further, compensation for grain growth has served to emphasize the exponential nature of the dependence of creep rate on density. The functional dependence of creep rate on density is commonly treated in terms of a stress intensity factor.

(ii) **Stress Intensity Factor:**

Eqn. 1 may also be written as

$$G^m = \dot{\varepsilon}\, K_1 \delta_a \phi^{(1+m/2)} \qquad \text{Eqn. (4)}$$

where K_1 is a constant at a fixed temperature, δ_a is the applied stress, ϕ is the stress intensity factor, with the exponent $p = 1$.

As seen in fig. 6, a plot of log $G^m\dot{\varepsilon}$ versus ρ or (1 - P), where P is the porosity , yields a single straight line for values of ρ between 0.5 and 0.9. This implies that within this range of ρ, ϕ depends only on the density (or porosity) and may indeed be expressed as

$$\phi = exp\ (aP) \qquad \text{Eqn (5)}$$

where a is a constant determined by the equilibrium dihedral angle The slope of log $(G^3\dot{\varepsilon})$ versus ρ gives $a = 1.6$

The exponential dependence of ϕ on ρ does not fit the Coble relation[3] $\phi = 1/\rho$ but has the functional dependence predicted by beere's model. However, $a = 1.6$ is a porosity dependence of ϕ that is

significantly weaker than the one predicted by Beere for the experimentally determined contact angle of ~120° for CdO. As pointed out by Viera and Brook,[6] the Coble relation may be more valid for $\rho >$ 0.9, i.e. the final stage of densification. Beere's model, on the other hand, gives too strong a dependence of ϕ on ρ to account fully for these results. A possible source of difference would arise when some fixed; substantial percentage of the pores would not lie in the grain boundaries. To reconcile the results, this fraction would need to be about 50%. The fraction of pores on the boundaries was not determined accurately. However, Fig. 5(A) would suggest that most pores do lie on boundaries. The lack of agreement may thus lie in other, as yet unidentified, factors.

(iii) **Densification Rate and Sintering Stress**

The curvature and the surface tension of the pores determine the rate at which matter is removed from a grainboundary for a particular geometry. The densification rate is then straightforwardly found from considering the stress distribution on the grainboundaries.[15] This leads, in 3-dimensions to a densification rate of the form:

$$\dot{\rho} = \frac{B\ D\ \Omega}{k_B\ T}\ \frac{1}{X_o^m}\ \Sigma \qquad \text{Eqn (6)}$$

where B is a geometrical constant and Σ is the driving force, or the sintering stress, and X_o is the neck radius, i.e, the square root of

the load bearing area between two grains. It is customary to put X_o proportional to the grain size. This is not correct, instead one has:

$$X_o = G\ (A_e/A)^{\frac{1}{2}} = G/\phi^{\frac{1}{2}} \qquad \text{Eqn (7)}$$

In analogy with the expression for creep, Eqn (1), one could then write

$$\dot{\rho} = \frac{BD\Omega}{k_B T}\ \frac{1}{G^m}\ \Sigma\phi^{m/2} \qquad \text{Eqn (8)}$$

Fig. 7 shows the logarithm of the observed densification rate, $\log \dot{\rho}$, versus the density, ρ, for the two green densities used. As found before for $\log \dot{\varepsilon}$, $\log \dot{\rho}$ decreases steeply and nearly linearly with increasing ρ. The creep-sintering experiments led to the conclusion that grain boundary diffusion is the dominant transport mechanism. At the low loads used the creep and densification should involve the same transport mechanism, so that the exponent m in Eqn. 1 and Eqn. 8 should be indentical. Using m=3 for the grainboundary diffusion, and the cubic growth law used to fit the results for the creep rate, a plot of $(G^3\dot{\rho}\phi^{-3/2})$ versus density, ρ, is also a plot of $\frac{BD\Omega\Sigma}{k_B T} = K'\Sigma$ versus p.

The equations for the creep rate and the densification rate may be written as

$$G^3\ \dot{\varepsilon} = K_1'\ \delta_a\ \phi^{5/2} \qquad \text{Eqn (10)}$$

$$G^3\ \dot{\rho} = K_2'\ \Sigma\phi^{3/2} \qquad \text{Eqn (11)}$$

where K_1' and K_2' are constants at a fixed temperature. The actual magnitude of the sintering stress, Σ, can be calculated from the densification results since it is reasonable to assume that $K_1' \approx K_2'$. Using this assumption, Σ is plotted versus ρ in fig. 8, for the compacts of green densities of 0.39 and 0.58 respectively. For both curves, Σ decreases slightly with increasing ρ, because of pore (grains) coarsening. For a given grain size, however, Σ increases with density, as indicated in fig 8. The results of Gregg and Rhines[8] for copper powder compacts, where Σ was found to increase with ρ up to ~ 0.95, may now be understood if grain growth is minimal or absent. The decrease in Σ for $\rho \gtrsim 0.95$ observed by Gregg and Rhines may be due to pore (grain) growth in their final stage.

Σ is also equal to γ/κ, where κ is the average curvature of the pore surfaces at the grain boundaries. It is interesting to consider Σ in light of the Zener relationship,[16]

$$r = \beta GP \qquad \text{Eqn (12)}$$

where β is a geometrical factor that is nearly equal to 1, and r is the pore radius. This relationship was approximately observed in CoO by Miro and Notis.[17] If it is assumed that in the intermediate stage $\kappa = 1/r$, then one could write

$$\frac{r}{G} = \frac{\gamma}{\Sigma G} \qquad \text{Eqn (13)}$$

A plot of $1/(\Sigma G)$ versus P should thus be a straight line according to the Zener relationship. Such a plot is shown in fig 9.

It is observed that the simple Zener relationship is a resonable approximation of the relationship between pore radius, r, grain size, G, and porosity, P, for wide density range.

(v) **Further Considerations:**

It was shown recently[2] that the application of low, uniaxial loads, although not affecting the overall volumetric densification rate, causes a small microstructural bias in the powder compact. The observed effect of this bias is shown in figure 10, where for example Curve B, sintered initially under 5N load, has a lower axial shrinkage rate than Curve C (sintered under no load) when the load is removed. The more detailed study undertaken in this paper, allows a possible interpretation of this hysteresis effect. Use is made of a simplified model, fig. 11, showing the grain boundaries in a porous compact subjected to an external, uniaxial load. Boundaries may be under compression, under tension, or sliding.

The creep process is viewed, on the basis of the results of this paper, as a series process in which sliding is accomodated by grain boundary diffusion. In the model, the diffusion path is likely to be along the grain boundary under compression to the neighbouring pore A, and from pore B along the grain boundary under tension, as indicated, thus preserving constant volume deformation. The microstructural bias introduced by this uneven redistribution of mass is likely to be in the geometry of the pores (and/or boundaries). The net effect is that the compact behaves as if it were denser in the direction of the applied

load, i.e. in the axial direction. Removal of the load then causes the compact to shrink slower in the axial direction, compared with the compact sintered under no load, but faster in the radial direction, as is observed.

Application of load to a compact, sintering initially under no load, leads to the opposite effect. This compact behaves as if it were less dense in the axial direction, compared with the compact sintered under load, and the axial shrinkage rate is higher (figure 10, Curves A and D).

Conclusions

The loading dilatometer has the great advantage of allowing the observation of simultaneous creep and sintering. When the data are considered together with volumetric density measurements, the contributions of creep and densification can be separated.

The creep measurements permit the determination of the stress intensity factor, ϕ , which is found to depend exponentially on the porosity over a wide density range.

The stress intensity factor, ϕ, enters into the expression for densification and permits the determination of the sintering stress, .

The sintering stress, Σ , decreases with increasing density when grain growth occurs. Its absolute value may be estimated if it is reasonably assumed that the kinetic constants for creep and sintering are the same.

The Zener relationship describes the pore size, grain size, and porosity relationship adequately in a wide density range.

The results for CdO at 1123K, show that grainboundary diffusion is the dominant transort mechanism.

Acknowledgement:

The authors wish to thank R. M. Cannon and A. G. Evans for some stimulating discussions.

References

1 A. G. Evans, "Considerations of Inhomogeneity Effects in Sintering," J. Amer. Ceram. Soc., 65 10 497-501 (1982).

2 M. N. Rahaman and L. C. De Jonghe, "Sintering of CdO Under Low Applied Stress:," J. Amer. Ceram. Soc., to be published.

3 R. L. Coble, "Diffusion Models for Hot Pressing with Surface Energy and Pressure Effects as Driving Forces," J. App.. Phys., 41 12 4798-4807 (1970).

4 W. Beere, "A Unifying Theory of the Stability of Penetrating Liquid Phases and Sintering Pores," Acta Metall., 23 1 131-38 (1975).

5 W. Beere, "The Second Stage Sintering Kinetics of Powder Compacts," ibid.,23 1 139-45 (1975).

6 J. M. Viera and R. J. Brook, "Kinetics of Hot-Pressing: The Semilogarithmic Law," J. Amer. Ceram. Soc., 67 4 245-49 (1984).

7 R. Raj and R. K. Bordia, "Sintering Behaviour of Bimodal Powder Compacts," Acta Metall., 32 7 1003-19 (1984).

8 R. A. Gregg and F. N. Rhines, "Surface Tension and the Sintering Force in Copper," Metall. Trans., 4 5 1365-74 (1973).

9 F. N. Rhines and R. T. De Hoff, "Channel Network Decay in Sintering," Mater. Sci. Res., 16, 49-61 (1984).

10 L. C. De Jonghe and M. N. Rahaman, "A Loading Dilatometer," Rev. Sci. Instr., to be published.

11 R. Raj, "Separation of Cavitation - Strain and Creep - Strain During Deformation," J. Amer. Ceram. Soc., 65 3 C-46 (1982).

12 F. R. N. Nabarro, "Deformation of Crystals by the Motion of Single Ions," Rep. Conf. on Strength of Solids, Bristol, 1947, 1948, pp 75 - 90.

13 C. Herring, "Diffusional Viscosity of a Polycrystalline Solid," J. Appl. Phys., 21 5 437-45 (1950).

14 R. L. Coble, "A Model for Boundary Diffusion Controlled Creep in Polycrystalline Materials," ibid., 34 6 1679-82 (1963).

15 C. H. Hseuh and L. C. De Jonghe, J. Amer. Ceram. Soc., to be published.

16 C. S. Smith, "Grains, Phases and Interfaces: An Interpretation of Microstructure," Trans. AIME, 175 15-51 (1948).

17 A. Miro and M. R. Notis, "Quantitative Image Analysis of Mirostructure Development During Pressure Sintering of CoO", Mater. Sci. Res. 13 457-469 (1979).

List of Figures

Figure 1. Axial shrinkage versus time for CdO compacts of two different green densities sintered under low applied loads (in newtons) at 1123K.

Figure 2. Axial shrinkage versus radial shrinkage for compacts of two different green densities sintered under the loads shown in newtons.

Figure 3. Creep strain versus time for loads shown in newtons.

Figure 4. Relative density versus time.

Figure 5 Scanning electron micrographs of the fracture surfaces of compacts (green density = 0.58) sintered for (A), t = 20 and (B), t = 120 min.

Figure 6. Dependence of the creep rate, , and the grain size compensated creep rate, $G^3\dot{\varepsilon}/G_o^3$ on relative density for densities 0.39 and 0.58 at three loads shown in newtons.

Figure 7. Densification rate, $\dot{\rho}$, and the grain size compensated densification rate, $G^3\dot{\rho}/G_o^3$ versus relative density.

Figure 8. The sintering stress versus relative density for compacts of two green densities.

Figure 9. Reciprocal of (sintering stress times grain size) versus porosity.

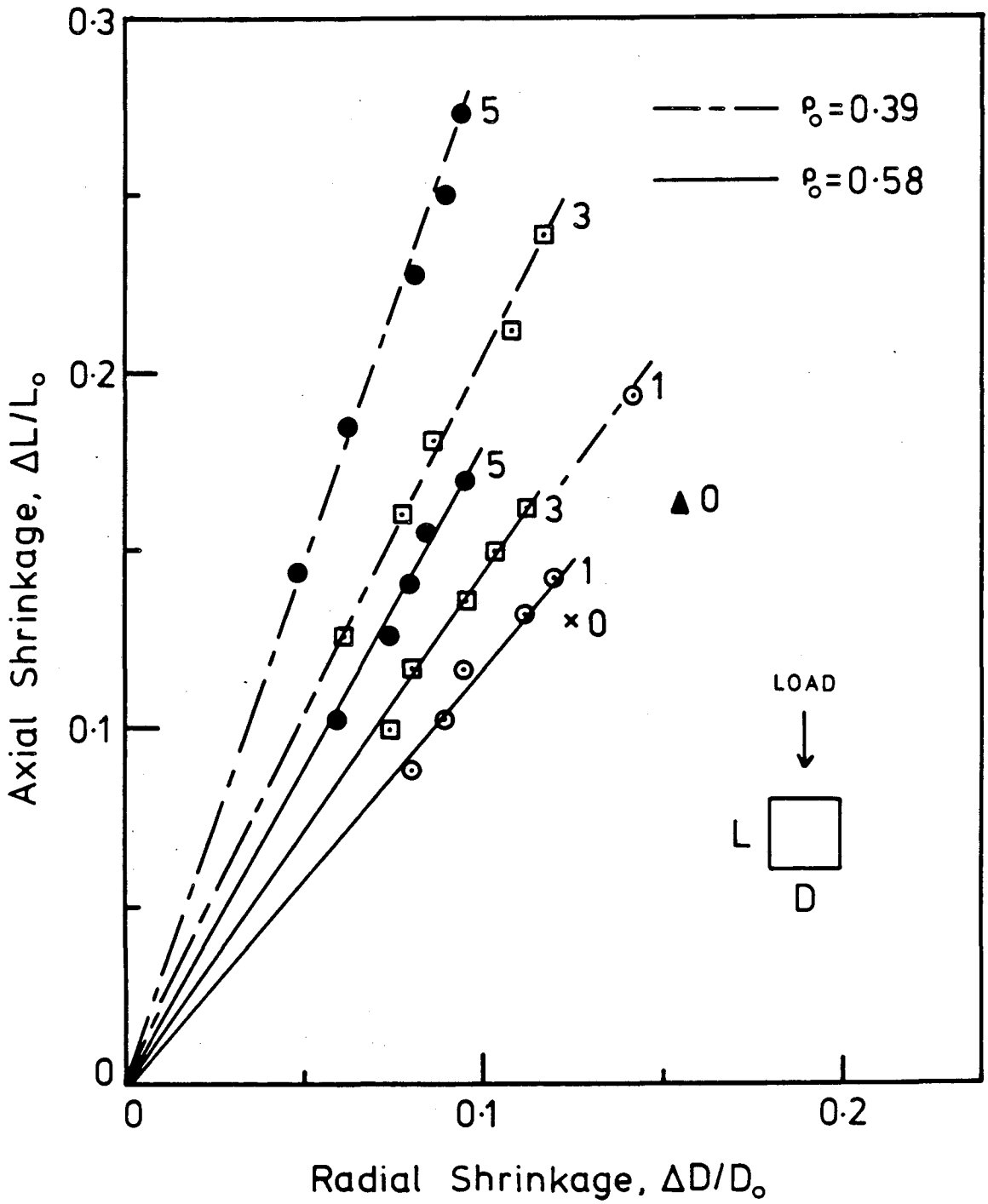

XBL 8411-4650

Figure 2.

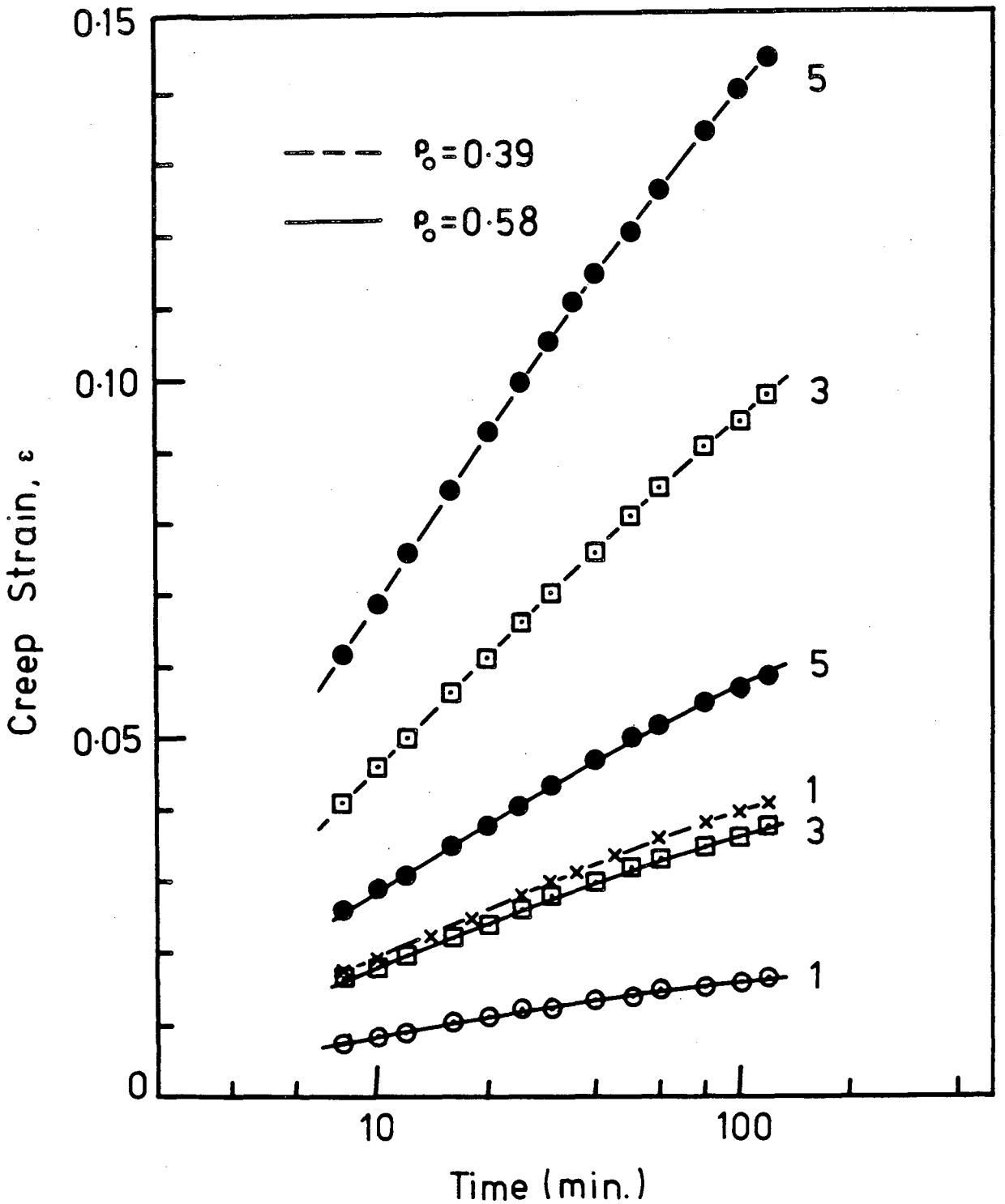

XBL 8411-4651

Figure 3.

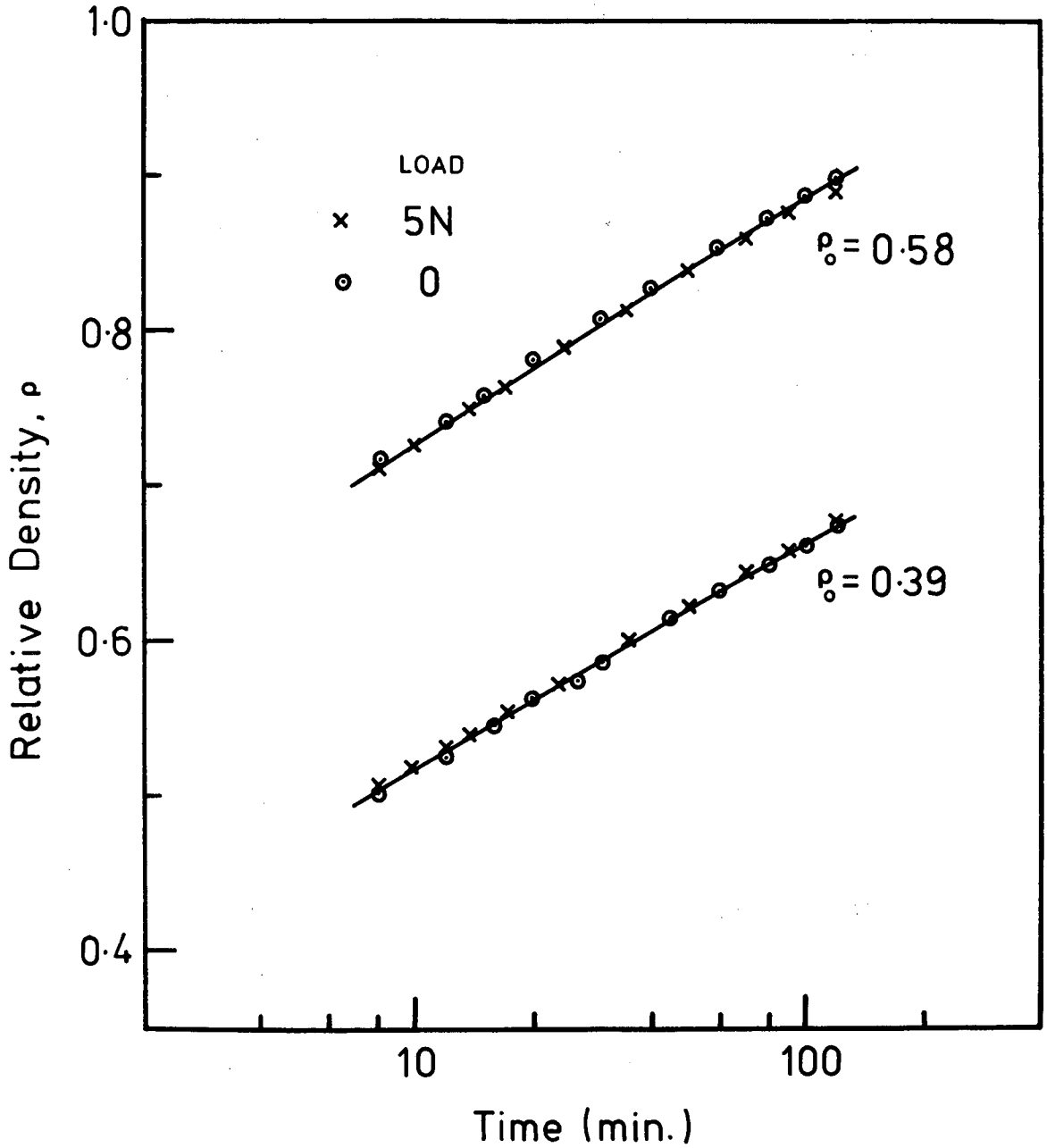

XBL 8411-4652

Figure 4.

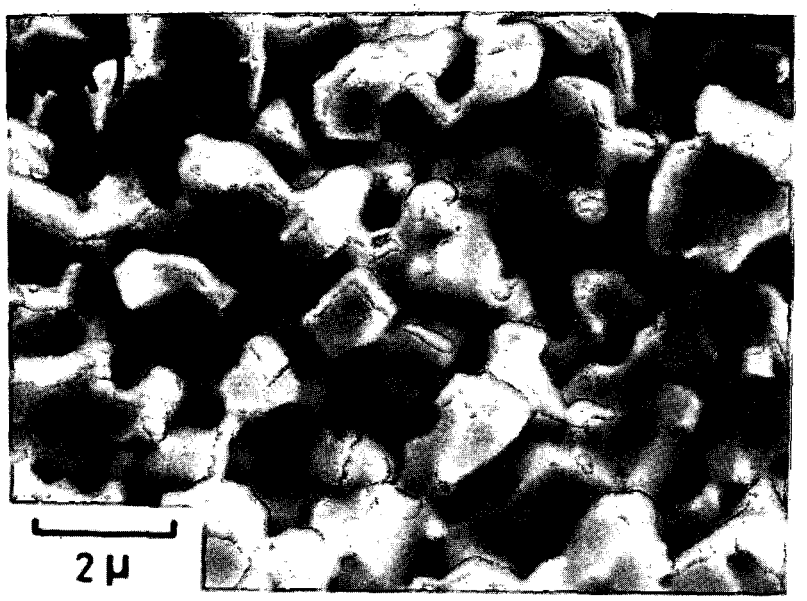

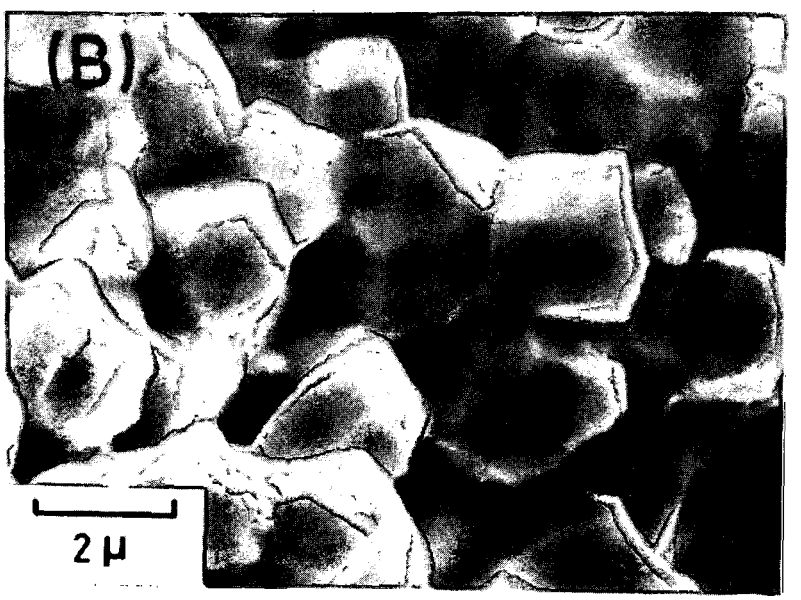

XBB 840-8476

Figure 5.

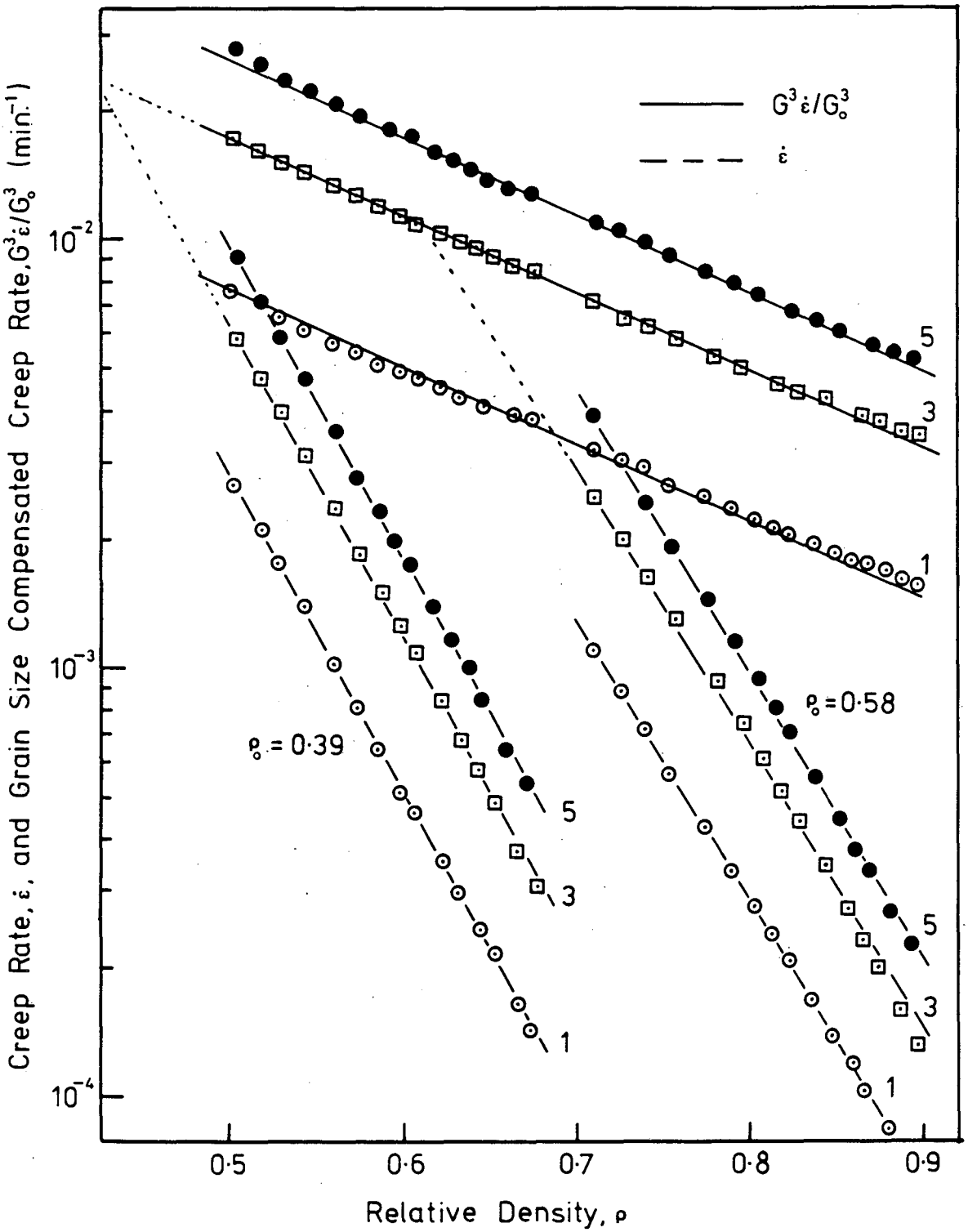

XBL 8411-4654

Figure 6

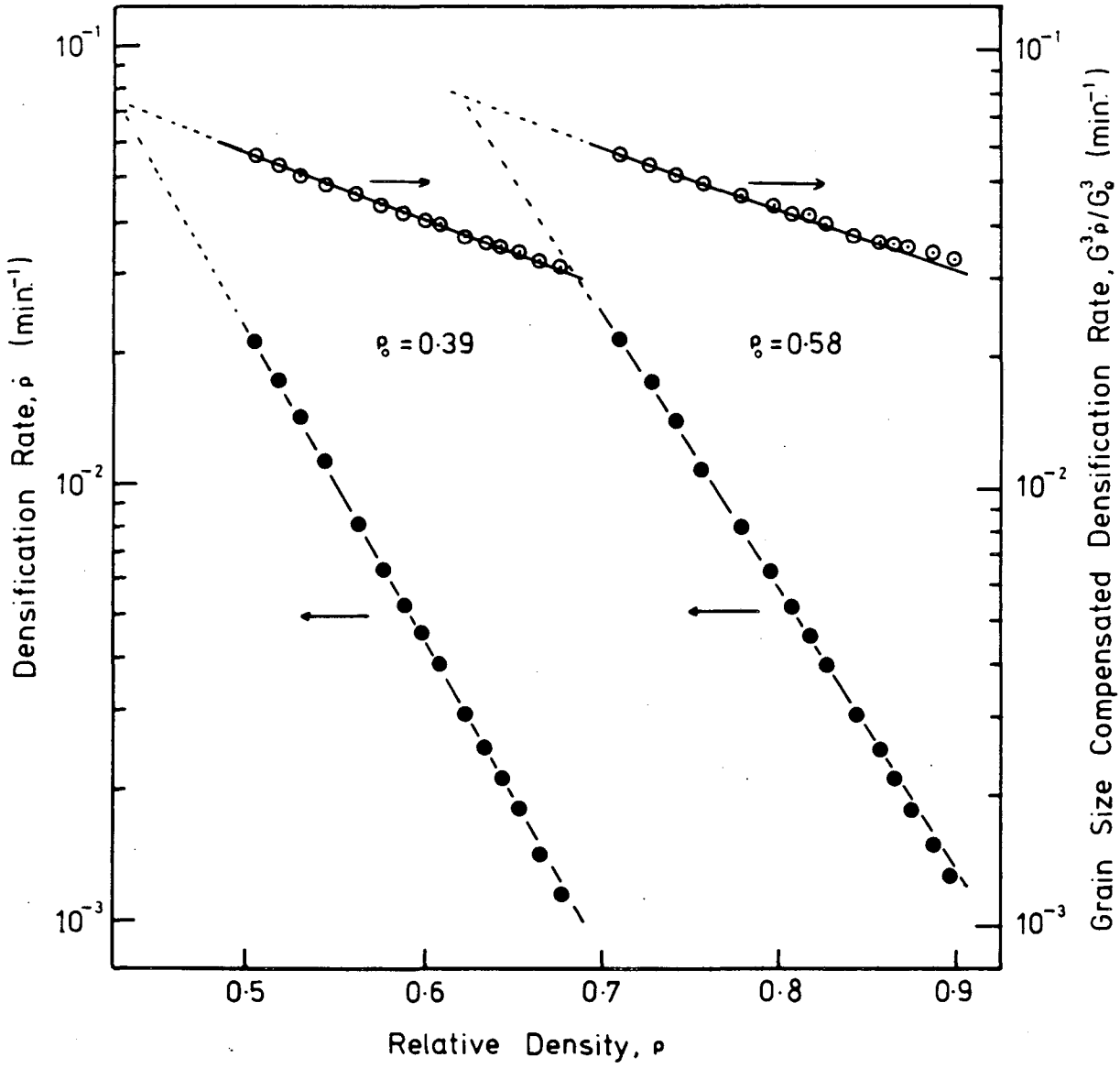

XBL 8411-4655

Figure 7

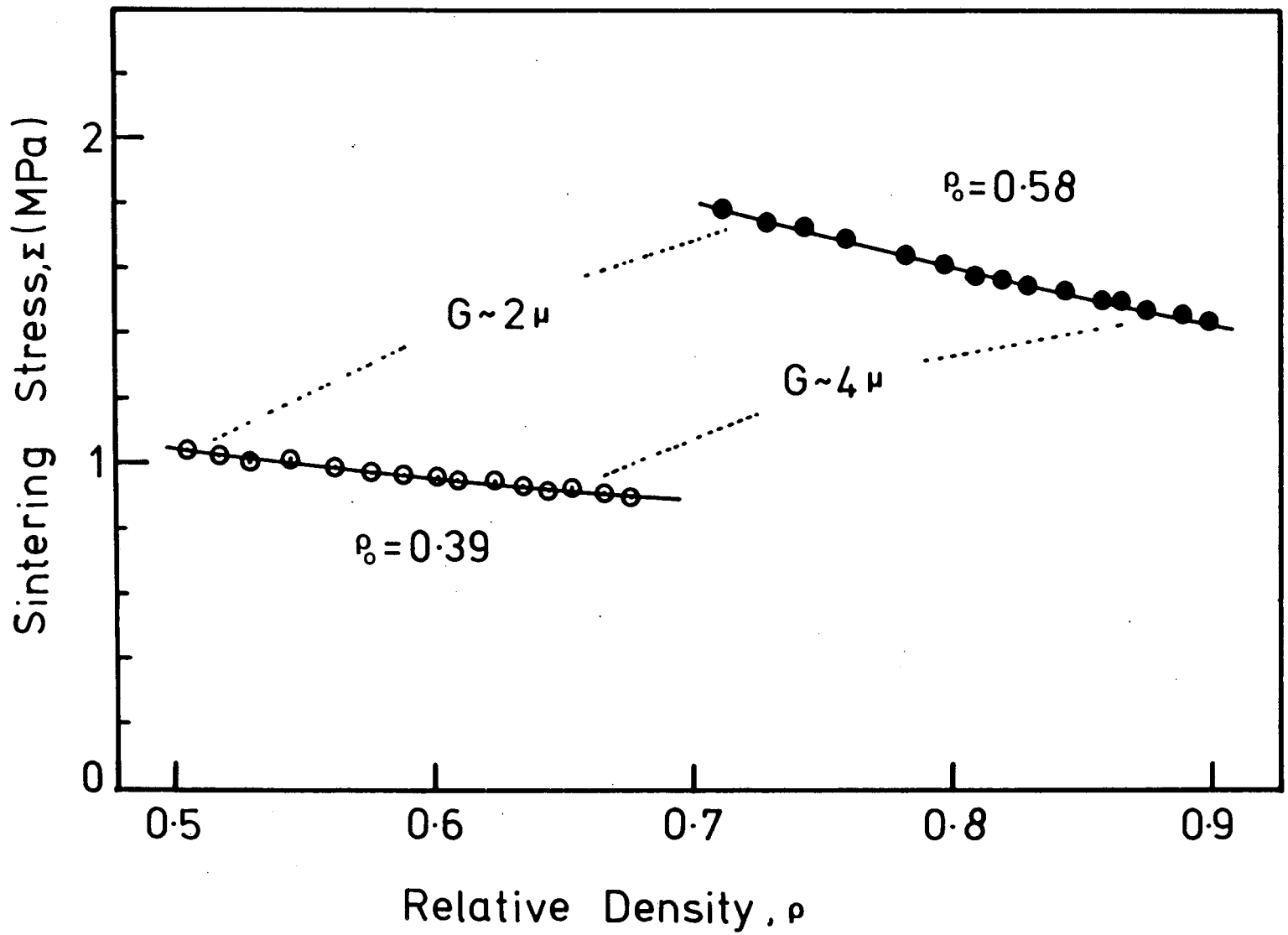

XBL 8411-4656

Figure 8

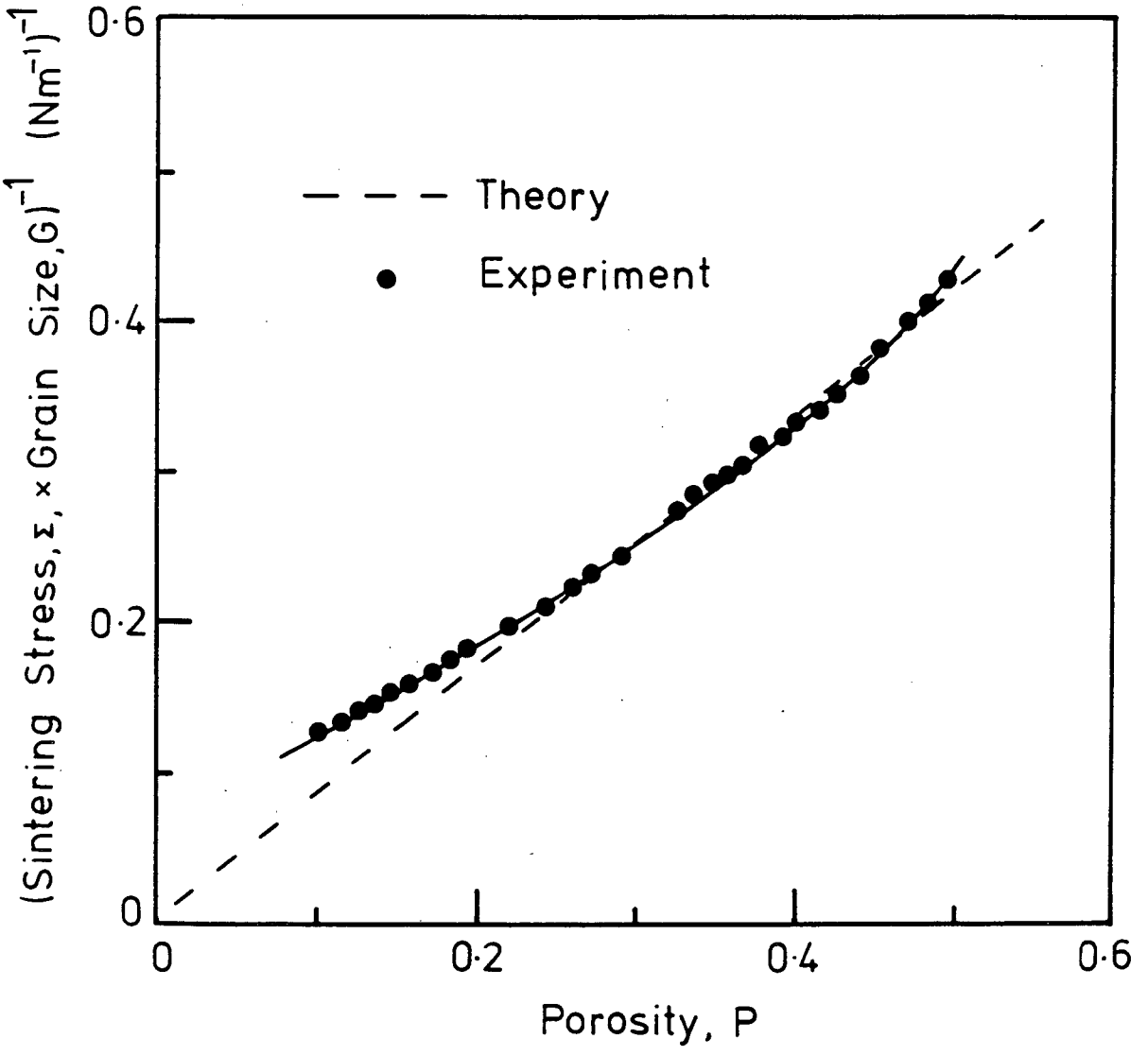

XBL 8411-4657

Figure 9

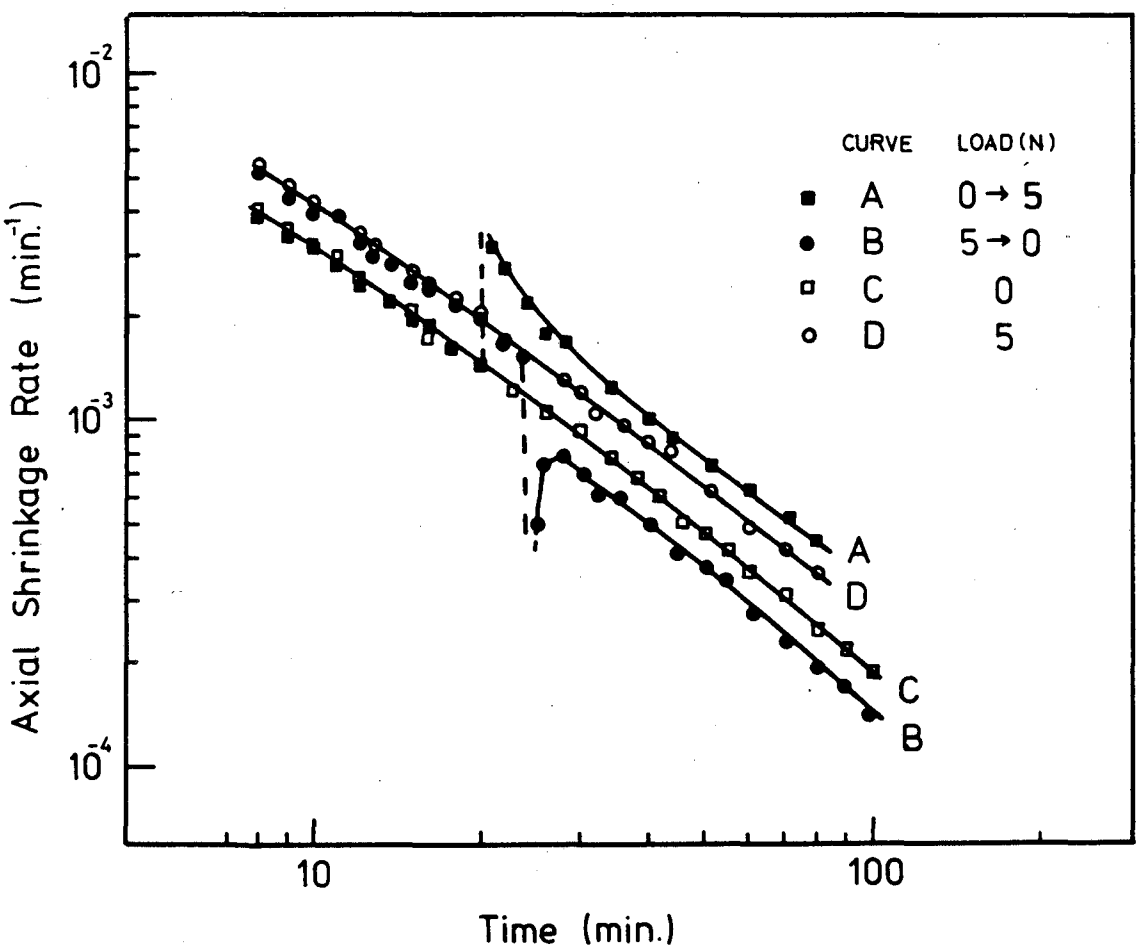
CURVE
LOAD (N)
A
0 → 5
B
5 → 0
C
0
D
5
A
D
C
B
Axial Shrinkage Rate (min.$^{-1}$)
10^{-2}
10^{-3}
10^{-4}
10
100
Time (min.)
XBL 847-2678

Figure 10

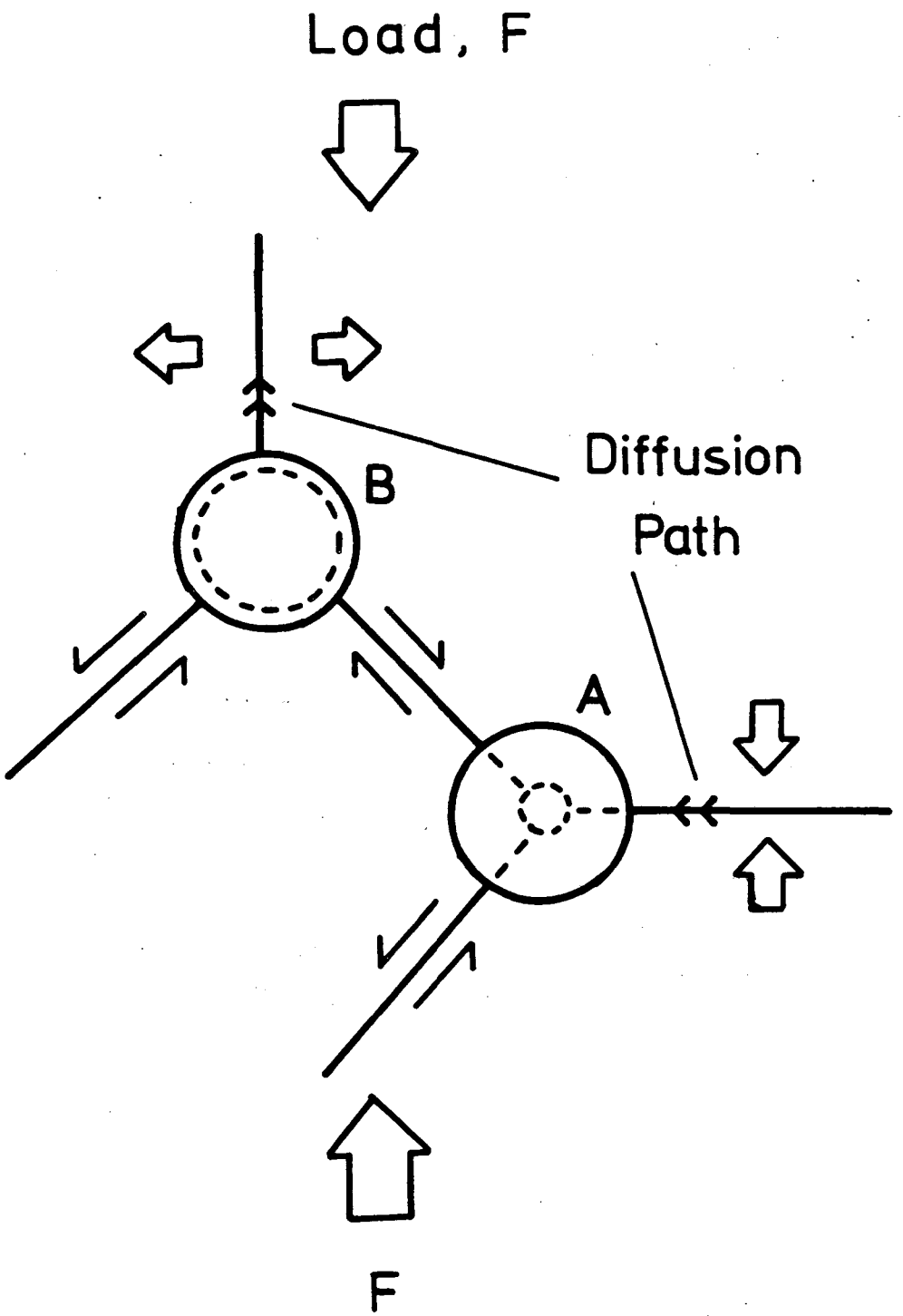

XBL 8411-4658

Figure 11

This report was done with support from the Department of Energy. Any conclusions or opinions expressed in this report represent solely those of the author(s) and not necessarily those of The Regents of the University of California, the Lawrence Berkeley Laboratory or the Department of Energy.

Reference to a company or product name does not imply approval or recommendation of the product by the University of California or the U.S. Department of Energy to the exclusion of others that may be suitable.

TECHNICAL INFORMATION DEPARTMENT
LAWRENCE BERKELEY LABORATORY
UNIVERSITY OF CALIFORNIA
BERKELEY, CALIFORNIA 94720